



JMRA

Journal of Mechanical Research and Application

ISSN: 2251-7383, eISSN: 2251-7391



A Deep Survey upon the Synthesis of AuS Nanostructures

Kouros Motevalli^{1*}, Zahra Yaghoubi²

^{1*} Applied Chemistry Department, South Tehran Branch, Islamic Azad University, Tehran, Iran

² IT Department, South Tehran Branch, Islamic Azad University, Tehran, Iran

Abstract. In this research, the dendritic gold(I) sulfide nanostructures were successfully synthesized by a simple hydrothermal route. The effect of temperature, and reaction time, on the morphology and particle dimension was also investigated. Thus, the efficiency of synthesized gold sulfide nanostructures in thin-film solar cells was evaluated. The results indicated very well that the particle dimension and morphology have effect on solar cells efficiency and dendritic gold sulfide nano-structures have higher efficiency compared to spherical and rod-like gold sulfide nanostructures. Moreover, depositing of dendritic gold sulfide upon gold sulfide nanoparticles led to obtaining 3.28% cell efficiency that in comparison with sole dendritic nanostructures and sole nanoparticles (1.89%), efficiency improvements of 48 and 85% were, respectively, obtained and also this important point must be elucidated that these nanostructures are useful for mechanical usages especially in manufacturing some linked rings in water treatment installations. Also, if we want to be decided for comparing with similar works presented for gold sulfide preparation [1–10], then, this fact will be illuminated easily that we synthesized dendritic gold sulfide nano-structures using new initiating reagents and without using surfactants by an easy route which can be more able in solar cells. In other words, the effect of morphology upon solar cell capability was learned about, and applying novel and appropriate approach in cell provision, essential advancement in cell was achieved.

Key Words: synthesis, nanostructure, hydrothermal, semiconductor

1. Introduction

Gold(I) sulfide, a *p*-type semiconductor with a bulky bandgap of 1.24 eV which is in the best acceptable range for solar-energy conversion [1–4], can be used in solar cells [2–8], photocatalysts [9], catalysts [10], biosensors [11], nanoscale switches [12], and cold cathodes [13]. Hence, many studies have focused upon seeking an easy method for synthesis of Silver sulfide nanostructures such as nanoparticles [2, 14, 15], nanowires [16], nanorods [17], nanoplates, dendrites, and hollow microspheres. Different chemical methods such as solvothermal, hydrothermal [20], ultrasonic [6], microwave [4], and co-sedimentation [1] have been

* Corresponding author e-mail: kmotevalli451@gmail.com

used to synthesize this substance. As seen these facts, dendrites, as a sort of fractal structure, which are generally created by chemical self-assembly under nonequilibrium conditions, have received intensive profit in recent years [18,19].

2. Experimental

2.1 Methods

All of the applied chemicals in this work were of analytical grade and used as-received without any further purification. Fourier transform infrared (FT-IR) spectra were recorded upon Magna-IR, spectrometer 550 Nicolet with 0.127 cm^{-1} resolution in KBr pellets in the range of $400\text{--}4000\text{ cm}^{-1}$. Scanning electron microscopy (SEM) images were obtained on LEO-1455VP equipped with an energy dispersive X-ray spectroscopy. Photocurrent density–voltage (J–V) curve was measured using computerized digital multimeters (Ivium-n-Stat Multichannel potentiostat) and a variable load. A 400 W metal xenon power source (Luzchem) applied as assimilated sun light source, and its light intensity (or radiant power) was adjusted to simulated AM 1.8 radiation at 118 mW/cm^2 with a filter for this purpose.

2.2 Preparation of $[\text{Au}(\text{en})_2(\text{H}_2\text{O})_2]\text{Cl}$

Firstly, 2 mmol of ethylenediamine (en) was added drop-wise to an AuNO_3 solution (1 mmol in 50 ml of distilled water). Then, the mixture was stirred and heated at $66\text{ }^\circ\text{C}$ for 1 h. Finally, the obtained sediment was centrifuged, washed with methanol and ether as the most effective solvents several times, and dried at $62\text{ }^\circ\text{C}$.

2.3 Synthesis of dendritic gold sulfide nanostructures

In a typical experimental procedure, 2 mmol of $[\text{Au}(\text{en})_2(\text{H}_2\text{O})_2]\text{Cl}$ and 1 mmol of cysteine were mixed in 30 ml of distilled water and stirred for 18 minutes. The final solution was poured to the 200 ml Teflon-lined stainless steel autoclave maintained at $158\text{ }^\circ\text{C}$ for 10 h, and then, the autoclave was permitted to being cooled to room temperature virtually. The resulting black sediment was gathered and then washed with ethanol as suitable polar solvent and distilled water for several times and was dried at $73\text{ }^\circ\text{C}$ for 13 h (sample A2). The effects of temperature, time of reaction, and cysteine concentration were also investigated. Reaction cases are listed in Table 1.

Table 1 The reaction conditions for gold(I) sulfide nanostructures

Sample no.	Temperature ($^{\circ}\text{C}$)	Time (h)	Au source: cysteine ratio	Morphology
1	105	10	2:1	Dendritic
2	157	10	2:1	Dendritic
3	207	10	2:1	Nanorod
4	158	10	2:1	Dendritic
5	157	23	2:1	Dendritic
6	155	18	4:1	Nanoparticle/dendritic
7	155	10	1:1	Nanosheet

3. Results and discussion

two absorption bands located at 3375 and 3245 cm^{-1} are related to N–H stretching of primary amine ($-\text{NH}_2$) and two bands at 2955 and 2895 cm^{-1} correspond to $-\text{CH}_2$ asymmetric and symmetric stretching cases [20]. The absorption band at 1585 cm^{-1} is dedicated for N–H bending of $-\text{NH}_2$, the band at 1054 cm^{-1} is related to C–N stretching state, and the bands at 689 and 534 cm^{-1} correspond to Au–N and Au–O stretching vibrations [18,19]. The FTIR results indicate that the $[\text{Au}(\text{en})_2(\text{H}_2\text{O})_2]\text{Cl}$ complex was well formed. Figure 1b represents FTIR spectrum of synthesized dendritic gold sulfide nanostructures. Since the curve in this condition has no absorption peaks, pure gold sulfide nanostructures were synthesized without any organic impurities. The effect of temperature, reaction time, and the ratio of reactants on the morphology and particle dimension were examined by different experiments and the obtained products were verified using SEM images. For verifying temperature effect upon morphology, three experiments were conducted at 110 $^{\circ}\text{C}$ (sample A1), 160 $^{\circ}\text{C}$ (sample A2), and 210 $^{\circ}\text{C}$ (sample A3) and their SEM images are verified in Fig. 2a–c. As being indicated, at 110 $^{\circ}\text{C}$ for 10 h, the nanoparticles were self-assembled to form dendritic-like structures (Fig. 2a). By increasing temperature from 108 $^{\circ}\text{C}$ (sample A1) to 158 $^{\circ}\text{C}$ (sample A2), the particles were smaller and well-ordered and uniform dendritic nanostructures were produced (Fig. 2b). At higher temperatures in hydrothermal reaction, the nucleation rate is faster than growth rate and so smaller particles will be formed. When the temperature was increased to 112 $^{\circ}\text{C}$ (sample A3), morphology was changed and rod-like nanostructures with average diameter of 24–36 nm and average length of 114–298 nm were prepared (Fig. 2c). Therefore, reaction time of 10 h is optimum time for preparation of appropriate dendritic gold sulfide nanostructures at 158 $^{\circ}\text{C}$ (sample A2). Figure 2 is relevant to the effect of $[\text{Au}(\text{en})_2(\text{H}_2\text{O})_2]\text{Cl}$ /Cysteine mole ratio, and for this purpose, the ratio of 4:1 and 1:1 (in addition to the 2:1) was selected (samples A6 and A7, respectively). As is obvious,

in both cases, the morphology has altered and spherical nanoparticles and nanosheets, respectively, have been synthesized.

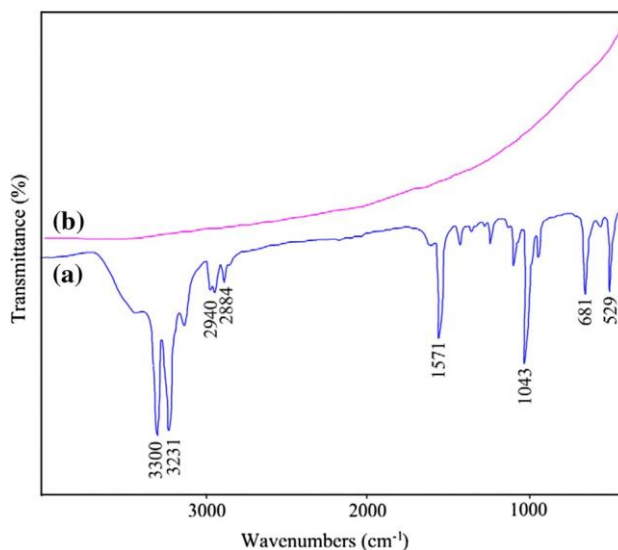


Fig. 1 FT-IR spectra of **a** [Au(en)₂(H₂O)₂]Cl and **b** dendritic gold sulfide nanostructure (sample A2)

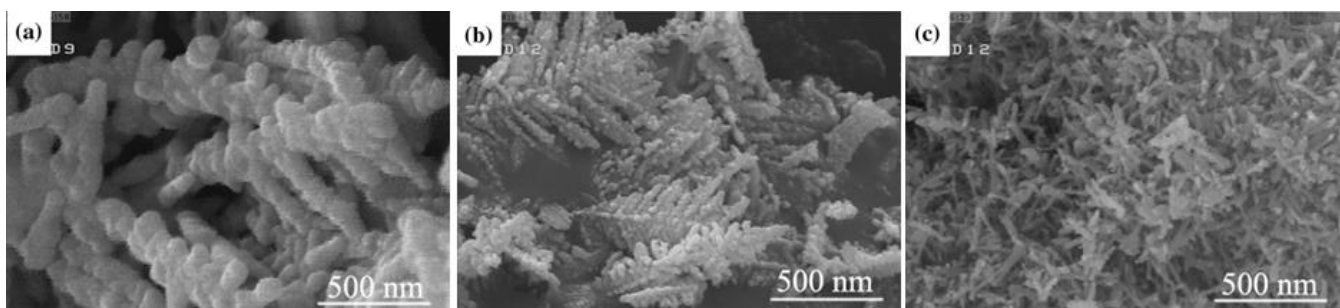


Fig. 2 SEM images of the synthesized gold(I) sulfide for 10 h at different temperatures **a** 108 °C (sample A1), **b** 158 °C (sample A2), and **c** 112 °C (sample A3)

Before the hydrothermal process, the production rate of sulfide from cysteine is very low and the formation of (gold sulfide)_m(Au(SCH₂CH(NH₂)COOH)₂)_{k/2} complex is so limited.

In comparison with similar works presented for gold sulfide preparation [1–10], we prepared dendritic gold sulfide nano- structures using new starting reagents and without using surfactants by a simple route which can be more capable in solar cells. Moreover, effect of morphology on solar cell efficiency was investigated, and using modern and suitable approach in cell preparation, important improvement in cell was obtained.

4. Conclusions

As summarized phrases, this fact should be said that dendritic-like, rod-like, and sheet-like Silver sulfide nanostructures were synthesized by a facile hydrothermal method using new starting reagents including $[\text{Au}(\text{en})_2(\text{H}_2\text{O})_2]\text{Cl}$ and cysteine. In accordance with our knowledge, this is the first time that the characterization of the synthesized gold sulfide nano- structures was carried out using SEM and FT-IR. Afterwards, the conduct of obtained nanostructures in solar cells was verified. Our results displayed that morphology and dimension have remarkable effect on efficiency of cells and prepared dendritic gold sulfide nanostructures have the highest efficiency. Moreover, being sedimented of dendritic nanostructures upon nanoparticles created a 90% improvement in solar cell efficiency [16,21] for mechanical usages.

Acknowledgements. This research was supported by the Chemistry Research Center at Islamic Azad University, south Tehran branch.

5. References

1. H. Salaramoli, E. Maleki, Z. Shariatini, M. Ranjbar, J. Photo-chem. Photobio. A: Chem. **271**, 56 (2013)
2. M. Peng, L.L. Ma, Y.G. Zhang, M. Tan, Y. J.B. W. Yu, Mater.Res. Bull. **44**, 1834 (2009)
3. Z. Li, W. Chen, H. Wang, Q. Ding, H. Hou, J. Zhang, L. Mi, Z.Zheng, Mater. Lett. **65**, 1785 (2011)
4. H. Lee, S.W. Yoon, E.J. Kim, J. Park, Nano. Lett. **7**, 778 (2007)
5. T. Sakamoto, H. Sunamura, H. Kawaura, T. Hasegawa, T. Nakay-ama, M. Aono, Appl. Phys. Lett. **82**, 3032 (2003)
6. N.S. Xu, S.E. Huq, Mater. Sci. Eng. R **48**, 47 (2005)
7. X. Liu, X.L. Wang, B. Zhou, W.C. Law, A.N. Cartwright, M.T.Swihart, Adv. Funct. Mater. **23**, 1256 (2013)
8. L. Chen, Y. Zou, W. Qiu, F. Chen, M. Xu, M. Shi, H. Chen, (ThinSolid Films) **520**, 5249 (2012)
9. Z.P. Liu, D. Xu, J.B. Liang, J.M. Shen, S.Y. Zhang, Y.T. Qian, J.Phys. Chem. B **109**, 10699 (2005)
10. M.B. Sigman, A. Ghezlbash, T. Hanrath, A.E. Saunders, F. Lee,B.A. Korgel, J. Am. Chem. Soc. **125**, 16050 (2003)
11. Mehdi Mousavi Kamazani , Seyed Amin Shobeir , Reza Rahmatolahzadeh , kourosh motevalli , Appl.phys.A(2017)123.314
12. Y.B. Chen, L. Chen, L.M. Wu, Chem. Eur. J **14**, 11069 (2008)
13. 13, X. Li, H. Shen, J. Niu, S. Li, Y. Zhang, H. Wang, L.S. Li, J. Am. Chem. Soc. **132**, 12778 (2010)
14. Y. Xiao, J. Chen, S.Z. Deng, N.S. Xu, S. Yang, J. Nanosci. Nano-technol. **8**, 237 (2008)
15. Z. Wu, C. Pan, Z. Yao, Q. Zhao, Y. Xie, Cryst. Growth Des. **6**,1717 (2006)
16. Q. Han, K. Xu, Mater. Lett. **85**, 4 (2012)
17. Y.F. Zhu, D.H. Fan, W.Z. Shen, Langmuir **24**, 11131 (2008)
18. M. Mousavi-Kamazani, M. Salavati-Niasari, M. Sadeghinia, Superlattice. Microst. **63**, 248 (2013)
19. S. Gorai, D. Ganguli, S. Chaudhuri, **59**, 826 (2005)
20. O. Amiri, M. Salavati-Niasari, M. Sabet, D. Ghanbari, Mater. Sci. Semicond. Process. **16**, 1485 (2013)
21. M. Sabet, M. Salavati-Niasari, D. Ghanbari, O. Amiri, M. Yousefi, Mater. Sci. Semicond. Process. **16**, 696 (2013)